Fundamental investigation on the development of composite membrane with a thin ion gel layer for CO_2 separation

Zhang, Jinhui ; Kamio, Eiji ; Matsuoka, Atsushi ; Nakagawa, Keizo ; Yoshioka, Tomohisa ; Matsuyama, Hideto

(Citation)
Journal of Membrane Science,663:121032

(Issue Date)
2022-12-05

(Resource Type)
journal article

(Version)
Accepted Manuscript

Fundamental investigation on the development of composite membrane with a thin ion gel layer for CO_2 separation

Jinhui Zhang [a,b], *Eiji Kamio* [a,b,c]*, *Atsushi Matsuoka* [a,b], *Keizo Nakagawa* [a,d], *Tomohisa Yoshioka* [a,d], *and Hideto Matsuyama* [a,b] *

[a]Research Center for Membrane and Film Technology, Kobe University, 1-1 Rokkodai-cho, Nada-ku, Kobe 657-8501, Japan

[b]Department of Chemical Science and Engineering, Kobe University, 1-1 Rokkodai-cho, Nada-ku, Kobe 657-8501, Japan

[c]Center for Environmental Management, Kobe University, 1-1 Rokkodai-cho, Nada-ku, Kobe 657-8501, Japan

[d]Graduate School of Science, Technology and Innovation, Kobe University, 1-1 Rokkodai-cho, Nada-ku, Kobe 657-8501, Japan

*To whom all correspondence should be addressed.

E-mail: e-kamio@people.kobe-u.ac.jp (E.K.)

E-mail: matuyama@kobe-u.ac.jp (H.M.)

ABSTRACT

A composite membrane with a thin defect-free ion gel layer was developed in this study. The ion gel layer containing an interpenetrating polymer network (IPN) and high ionic liquid (IL) content (80 – 90wt.%) was prepared on a poly(dimethylsiloxane) gutter layer by spin coating. The thickness of the IPN ion gel layer was reduced from 20 μm to 600 nm by increasing the dilution ratio of the ion gel precursor solution, and the CO_2 permeance of the composite membrane was increased from 45 to 613 GPU. By increasing the IL content of the IPN ion gel layer to 90 wt.%, the prepared composite membrane exhibited the CO_2 permeance of 778 GPU and CO_2/N_2 selectivity of 15. The CO_2 permeance and CO_2/N_2 permselectivity of the IPN ion gel layer alone having 90 wt.% IL were respectively estimated to be 1860 GPU and 27. The excellent gas permeation performance proves that IPN ion gel is a good optional material as a selective layer of a composite membrane for efficient CO_2 separation.

Keywords: Ion gel membrane, CO_2 separation, Composite membrane, Thin film preparation, High CO_2 permeance

1. Introduction

The prevention of global warming caused by the increase in the concentration of greenhouse gases, particularly CO_2, is an urgent issue for the mankind [1, 2]. To prevent the increase in the CO_2 concentration in the atmosphere, various CO_2 separation technologies have been developed. One promising technology is the membrane separation method, which requires less energy and cost for the operation than the other CO_2 separation methods such as absorption and adsorption [3–5].

However, for practical use, the CO_2 permeance of most CO_2 separation membranes remains insufficient. Therefore, the development of the membranes with high CO_2 permeance is highly desirable. One of the main restrictions for the development of the membrane with high CO_2 permeance is the insufficient CO_2 permeability of the membrane material. Thus far, significant efforts have been devoted to develop the membrane material with high CO_2 permeability, including polymer membranes with highly designed network configurations such as polymers with intrinsic microporosity and thermal rearrangement polymers, mixed matrix membranes, facilitated transport membranes, and ionic liquid (IL)-based membranes [6–16]. Among these membranes, IL-based membranes usually show excellent CO_2 permeability and have the advantage of easy tuning of the membrane performance by the selection of suitable IL for the application [13, 17]. If IL-based membranes could be fabricated in to thin films, very high CO_2 permeance of the membrane would be achieved.

ILs are nonvolatile and thermally stable liquid salts consisting of organic cations and

various kinds of anions. The physicochemical properties of an IL can be tuned by the design of the chemical structure as well as the selection of the cation and anion. By introducing some special structures such as fluoroalkyl groups in anions, alkyl-side chains and imidazolium groups in cations, some ILs are designed to have high CO_2 solubility [18-24]. For example, 1-ethyl-3-methylimidazolium bis-(trifluoromethanesulfonyl)imide ([Emim][Tf_2N]), 1-ethyl-3-methylimidazolium dicyanamide ([Emim][DCA]), and 1-ethyl-3-methylimidazolium tetracyanoborate ([Emim][$B(CN)_4$]), have a high solubility selectivity of CO_2 [24–26]. Additionally, ILs maintain a liquid state in a wide temperature range. It has been reported that the CO_2 diffusivity in an IL is normally higher than that in polymer materials [27–31]. Because the CO_2 diffusivity in polymer materials is strongly affected by the polymer chain motion, rigidity, entanglement and crosslinking of the polymer chains limit the polymer chain motion and the molecular motion of CO_2. On the other hand, because ILs are usually small molecule, the IL molecules easily move and the dissolved CO_2 can move together with the IL molecules. Therefore, the CO_2 diffusivity in an IL is generally higher than that in polymer materials. This high CO_2 solubility and diffusivity enables us to use the ILs as prospective candidates for high-performance CO_2 separation membranes [13, 32, 33]. An ion gel, which is a gel containing a large amount of an IL, is a quasi-solid material that can maximize the attractive properties of the ILs. The gas permeation property through an ion gel membrane with high IL content is determined by the property of the IL in the gel. As mentioned above, some ILs designed for CO_2 separation have high CO_2 solubility and diffusivity.

Thus, the ion gel-based CO_2 separation membranes have high CO_2 permeability and good permselectivity of CO_2 over other light gases [10–12, 34–38].

For the practical application of ion-gel-based membranes, ion gels should be made into a thin film to decrease the gas transport resistance and improve the gas permeance [14, 39, 40]. Until now, the fabrication of thin ion gel membranes has been challenging, because ion gels are generally weak materials with poor mechanical strength. Recently, however, tough ion gels, such as double-network ion gels [10–12, 35, 41–46], tetra-PEG ion gels [34, 47], ion gels with self-assembled copolymer networks [36, 37, 48], and ion gels with interpenetrating polymer networks (IPN) [49–51], have been developed. Among these tough ion gels, in this research, we focused on the use of our previously developed ion gel with IPN structure [51] because [Emim][Tf_2N], which is one of the CO_2-philic ionic liquids [24], can be used to prepare the tough ion gel. The prepared IPN ion gel membrane is composed of the poly(vinylidene fluoride-*co*-hexafluoropropylene) (PVDF-HFP) network, the poly(*N,N*-dimethylacrylamide-*co*-*N*-succinimidyl acrylate) (poly(DMAAm-*co*-NSA)) network, and over 80 wt.% of [Emim][Tf_2N].

In this study, a composite membrane with an ultra-thin IPN ion gel layer (600 nm) was prepared. The IPN ion gel layer was prepared on a poly(dimethylsiloxane) (PDMS) gutter layer using the spin-coating method. To increase the gas permeance of the composite membrane, the thickness of the IPN ion gel layer was reduced by increasing the dilution ratio of the IPN ion gel precursor solution. Additionally, the IL content of the IPN ion gel layer was increased to increase the CO_2 permeability of the ion gel layer, thereby

improving the separation performance of the composite membrane. A theoretical estimation of the gas permeation performance was also performed to demonstrate the excellent performance of the thin IPN ion gel layer of the developed composite membrane.

2. Experimental

2.1 Materials

Poly(vinylidene fluoride-*co*-hexafluoropropylene) (PVDF-HFP) pellets (Sigma-Aldrich) with M_w of 400000 g/mol and M_n of 130000 g/mol were used as the network material of the IPN ion gel. The other network material is poly(*N*,*N*-dimethylacrylamide-*co*-*N*-succinimidyl acrylate) (poly(DMAAm-*co*-NSA)) with *N*-succinimidyl acrylate (NSA) ratio of 2.91 mol% and M_n of 121 kg/mol, which was synthesized in accordance with the method described in our reported work [42, 46]. Diethylene glycol bis(3-aminopropyl) ether (DGBE) purchased from Tokyo Chemical Industry Co., Ltd. was used as the crosslinker of the poly(DMAAm-*co*-NSA). The IL 1-ethyl-3-methylimidazolium bis(trifluoromethanesulfonyl)imide ([Emim][Tf_2N]) was purchased from Tokyo Chemical Industry Co., Ltd. and used as received. It should be noted that the used ionic liquid ([Emim][Tf_2N]) cannot react with CO_2 so that the prepared IPN ion gel membrane is not the CO_2 facilitated transport membrane. Acetone (99.5 wt.%) purchased from FUJIFILM Wako Pure Chemical Co., Ltd. was used as the diluent for the IPN ion gel precursor solution. Sylgard 184 silicone elastomer base and curing agent purchased from Dow Silicones Co., Ltd. were used to prepare the PDMS gutter layer. Poly(sodium 4-

styrenesulfonate) (average M_w of ~70000, Sigma-Aldrich Co.) was used as a sacrificial layer for the preparation of the gutter layer.

2.2 Preparation of the IPN ion gel precursor solution

The precursor solution for the PVDF-HFP/poly(DMAAm-*co*-NSA) IPN ion gel was prepared by dissolving PVDF-HFP, poly(DMAAm-*co*-NSA), DGBE and [Emim][Tf_2N] in acetone. The schematic illustration of the preparation of the precursor solution is shown in Scheme 1. The detailed preparation procedures are described elsewhere [51]. In this study, the weight ratio of PVDF–HFP to the sum of IPN precursors (PVDF–HFP, poly(DMAAm-*co*-NSA), and DGBE) was fixed at 0.5 g/g, and the molar ratio of DGBE/NSA was fixed at 0.5 mol/mol. The precursor solutions of the IPN ion gels with different dilution ratios were prepared by changing the weight ratio of acetone to the sum of the IL and network precursors. This ratio was defined as *r* to indicate the dilution degree of the IPN ion gel precursor solution. A higher *r* value indicates a higher dilution ratio of the IPN ion gel precursor solution.

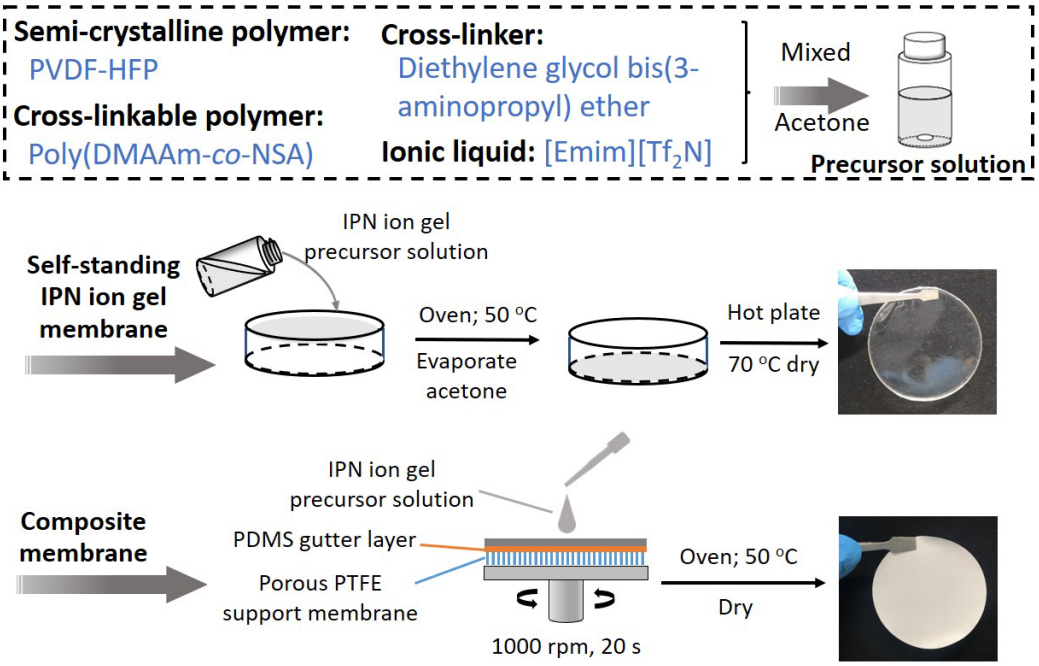

Scheme 1. Schematic illustrations of the preparation of the self-standing IPN ion gel membrane and the composite membrane containing the thin IPN ion gel layer.

2.3 Preparation of the support membrane

In the current stage, it is difficult to prepare a free-standing ion gel membrane with a thickness less than 100 μm. Therefore, in this study, a support membrane composed of a porous polytetrafluoroethylene (PTFE) membrane and a dense PDMS gutter layer was used as the substrate for the preparation of the thin ion gel membrane. The function of the PDMS gutter layer is to prevent the ion gel precursor solution from entering the pores of the PTFE membrane. The PDMS gutter layer was prepared by following the previously reported method [52, 53]. First, the glass plate was cleaned and treated for 5 min by air plasma (YHS-R, Kai Semi-conductor Co., Ltd.). Poly(sodium 4-styrenesulfonate) aqueous solution (30 wt.%) was spin-coated on the plasma-treated glass plate at the

147 rotation speed of 3000 rpm for 1 min using a spin-coater (MS-A100, Mikasa Co., Ltd.).
148 The glass plate with the poly(sodium 4-styrenesulfonate) layer was dried on a hot plate at
149 120 °C for 5 min. The base and curing agent of Sylgard 184 were mixed at a 10 : 1 mass
150 ratio and diluted by hexane to adjust the concentration to 5 wt.%. This solution was spin-
151 coated onto the glass plate with the poly(sodium 4-styrenesulfonate) layer at the rotation
152 speed of 4000 rpm for 1 min. It was then dried on a hot plate at 120 °C for 30 min to
153 perform the crosslinking reaction of the PDMS layer. A polytetrafluoroethylene (PTFE)
154 porous membrane (Toyo Roshi Kaisha, Ltd., Japan; pore size: 0.1 μm) was pasted onto
155 the PDMS layer and they were immersed in pure water. Because the poly(sodium 4-
156 styrenesulfonate) layer was dissolved in water, the PTFE membrane with the PDMS
157 gutter layer separated from the glass plate. The PDMS layer surface was then washed
158 with pure water to completely remove the residual poly(sodium 4-styrenesulfonate).
159 Finally, it was dried at ambient temperature. The prepared PDMS gutter layer without any
160 treatment had a CO_2 permeance of 1600 GPU and a CO_2/N_2 permselectivity of 5.61.
161

162 **2.4 Preparation and characterization of the self-standing IPN ion gel membrane**

163 The mechanical strength, surface morphology, and CO_2 and N_2 permeability of the IPN
164 ion gel membrane prepared with the precursor solution with different dilution ratios were
165 evaluated using thick self-standing IPN ion gel membranes. The schematic illustration of
166 the preparation of the self-standing IPN ion gel membrane is shown in Scheme 1. The
167 precursor solution was poured into an open mold and placed in an oven at 50 °C for 24 h

168 to roughly evaporate the diluent (acetone). Subsequently, the prepared self-standing IPN
169 ion gel membrane was dried completely on a hot plate at 70 °C for 24 h. The thickness of
170 the IPN ion gel membrane was determined by observing the cross-section of the
171 membrane using a digital microscope system (LEICA DMS300). The tensile strength of
172 the self-standing IPN ion gel was measured using a universal testing instrument (EZ-LX,
173 Shimadzu Co., Japan). The thickness of dumbbell-shaped IPN ion gel samples, measured
174 using the digital microscope system, was used to calculate the tensile stress. The tensile
175 strain was increased at the rate of 100 mm/min. The loading-unloading cyclic tensile test
176 was performed to evaluate the dissipated energy in response to the force application. In
177 the cyclic tensile tests, the strain increased by 0.5 mm/mm per cycle.
178
179 **2.5 Preparation of the composite membrane with thin IPN ion gel layer**
180 The thin-film preparation methods such as casting and roll-to-roll coating are simple
181 and easy for large-scale application. However, in the current stage of our research, it is
182 hard for us to prepare a large-scale composite membrane with a thin and defect-free ion
183 gel layer. The main target of this research is to confirm the CO_2 permeation performance
184 of the composite membrane with a thin and defect-free ion gel layer. Therefore, we
185 adopted a spin-coating method because it is a facile method to prepare a thin membrane
186 in a lab scale.
187 The CO_2 permeation performance of the thin IPN ion gel membrane was evaluated
188 using the composite membrane composed of thin IPN ion gel layer, PDMS gutter layer,

and porous PTFE support. The schematic illustration of the preparation of the composite membrane is shown in Scheme 1. The IPN ion gel precursor solution was spin-coated onto the support membrane with PDMS gutter layer at the rotation speed of 1000 rpm for 20 s. In this study, just before the use, the PDMS gutter layer was pre-treated by the air plasma for 2 s to improve the wettability of the precursor solution. After spin-coating the precursor solution, the composite membrane was dried in an oven at 50 °C for 24 h. The surface morphology and roughness of the IPN ion gel were measured using a laser microscope (KEYENCE, VK-X3000). The thickness of the IPN ion gel layer was measured using a field-emission scanning electron microscopy (FE-SEM JSM-7500F, JEOL Ltd., Japan). To control the thickness of the IPN ion gel layer, the precursor solutions with different dilution ratios were used. In addition, the precursor solution with large IL content was used to increase the IL content of the IPN ion gel layer. The compositions of the precursor solutions are shown in Table S1.

2.6 Evaluation of the gas separation performance

The CO_2/N_2 separation performance of the IPN ion gel membranes (self-standing and composite membranes) was evaluated using the sweep method with a permeation apparatus described elsewhere [35, 46]. The feed gas was a mixture of 50/50 mol/mol of CO_2 and N_2. It was fed into the gas permeation cell at the constant flow rate of 200 mL/min. The sweep gas (Helium) was fed to the permeation side of the gas permeation cell at the constant flow rate of 40 mL/min. The flow rates of the feed and sweep gases

were controlled using a mass flow controller (Hemmi Slide Rule Co., Ltd., Japan). The gas permeation test was conducted at 30 °C under atmospheric pressure. The compositions of the permeated CO_2 and N_2 in the sweep gas, measured using gas chromatograph (GC-8A, Shimadzu Co., Japan), were used to calculate the CO_2 and N_2 permeances.

3. Results and discussion

3.1 Effects of dilution ratio of the precursor solution on the mechanical properties and surface roughness of the IPN ion gel membranes

To prepare an ultra-thin ion gel layer, the ion gel should have a sufficiently high mechanical strength and low surface roughness [45]. In this study, an ultra-thin ion gel layer was prepared using a highly diluted precursor solution of the IPN ion gel. Prior to the preparation and evaluation of the composite membrane with an ultra-thin IPN ion gel layer, the effects of the dilution ratio of the precursor solution on the mechanical strength and surface roughness of the IPN ion gel were investigated. Self-standing IPN ion gel membranes were used for this investigation.

The mechanical properties of the IPN ion gels prepared using the precursor solutions with different *r* values were evaluated through uniaxial tensile tests. It should be mentioned that when the *r* values were higher than 12.8 g/g the prepared free-standing IPN ion gels were too thin to be measured for the uniaxial tensile test. The stress-strain curves of the IPN ion gels are presented in Fig. 1. As shown in Fig. 1, no clear dependence

of the mechanical properties on the *r* values was found. To further confirm this result, the Young's modulus, fracture stress, fracture strain, and fracture energy of the IPN ion gels were determined from uniaxial tensile stress–strain curves. At each *r* value, at least 4 ion gel samples were measured and the average values of the Young's modulus, fracture stress, fracture strain, and fracture energy were calculated and presented in Fig. S1. The results in Fig. S1 show that the mechanical properties are not dependent on the *r* value and approximately the same. This indicates that the dilution ratio of the precursor solution does not significantly affect the mechanical strength of the IPN ion gel.

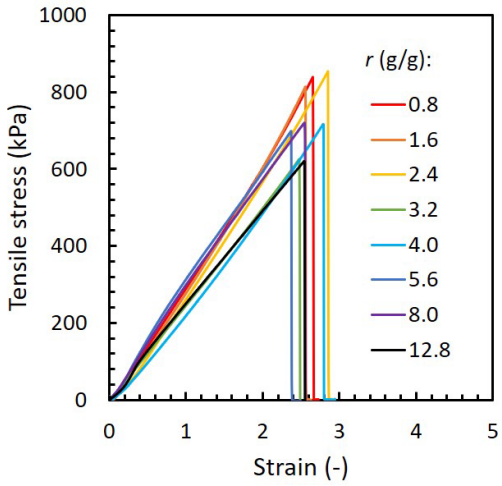

Fig. 1. Uniaxial tensile stress–strain curves of IPN ion gels as a function of the dilution ratio of the ion gel precursor solution. *r* is the weight ratio of acetone to the sum of the IL and network precursors in the precursor solution of the IPN ion gel. The IL content of the IPN ion gels was 80 wt.%.

Evaluating the surface roughness of the IPN ion gel prepared using a diluted precursor solution is also essential. When an external force is applied to an ion gel thin film, the stress is concentrated on the thin parts, leading the defect formation and making the ion

248 gel break easily. To avoid the defect formation in an ultra-thin ion gel layer of the
249 composite membrane, the ion gel layer should have a low surface roughness. Therefore,
250 the effects of the dilution ratio of the precursor solution on the surface roughness of the
251 IPN ion gel layer were investigated.

252 In this investigation, the IPN ion gel layer was prepared on a glass plate using the spin-
253 coating method. The IPN ion gel precursor solution was spin-coated at a rotation speed
254 of 1000 rpm for 20 s, then dried in an oven at 50 °C for 24 h. The surface roughness of
255 the prepared IPN ion gel layer is presented in Fig. 2. As shown in Fig. 2(a), the arithmetic
256 mean height (S_a) of the IPN ion gel thin layer decreases with increasing r values. A lower
257 S_a means that the gel surface is smoother. Therefore, when the dilution ratio of the IPN
258 ion gel precursor solution increases, the surface of the IPN ion gel layer tends to be
259 smoother (Fig. S2). The IPN ion gel layer prepared using the highly diluted precursor
260 solution with r equal to 24 g/g had a smooth surface, as shown in Fig. 2(b). This
261 characteristic is preferred for the preparation of a thin ion gel layer.
262

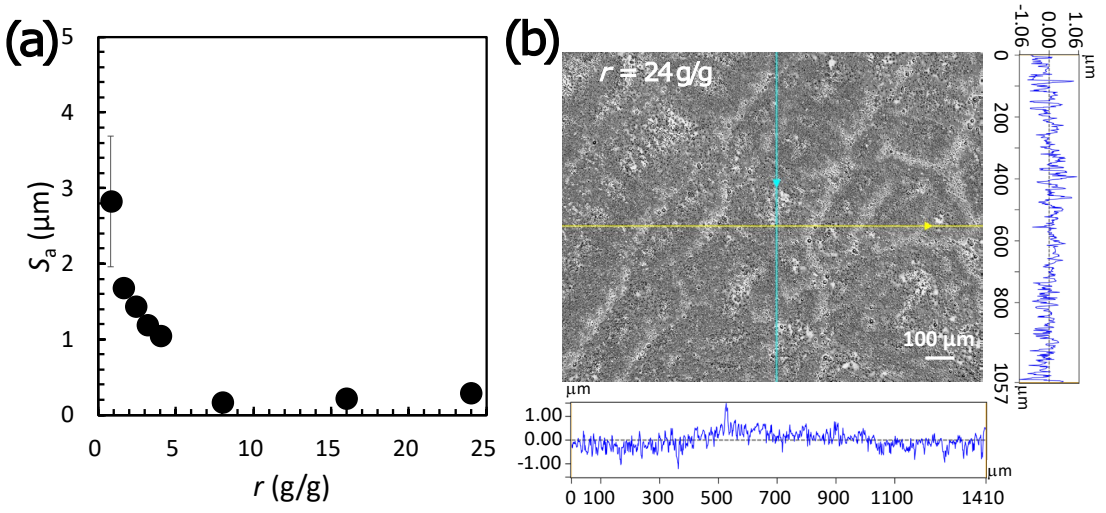

Fig. 2. Effects of dilution ratios of precursor solution on the surface roughness of IPN ion gel containing 80 wt.% of the IL. (a) Relationship between the arithmetic mean height (S_a) of the IPN ion gel layer and the dilution ratio (r) of the precursor solution. (b) Surface morphology and roughness curves in horizontal and vertical directions of the IPN ion gel layer prepared using the precursor solution with r equal to 24 g/g.

3.2 Effects of dilution ratio of precursor solution on the gas permeation property of IPN ion gel membranes

To develop a highly and selectively CO_2 permeable composite membrane with an ultra-thin IPN ion gel layer, the ion gel layer should have high CO_2 permeability and high CO_2/N_2 selectivity. Regarding the CO_2 permeation property, it was concerned that the dilution of the precursor solution of the IPN ion gel layer would affect to the CO_2 permeability and CO_2/N_2 selectivity. Therefore, the effect of the dilution ratio of the precursor solution on the gas separation performance of IPN ion gel membranes was investigated. In this investigation, the CO_2 and N_2 permeabilities were evaluated using thick self-standing IPN ion gel membranes prepared from precursor solutions with different dilution ratios. The results are presented in Fig. 3. As shown in Fig. 3(a), the

281 CO_2 permeabilities and CO_2/N_2 selectivities are almost constant at different *r* values. This
282 indicates that the dilution ratio of the precursor solution does not significantly affect the
283 gas permeation property of the IPN ion gel. This result is preferable for the preparation
284 of ultra-thin IPN ion gel layers using diluted precursor solutions. Additionally, the CO_2
285 permeance exhibits proportional relationship with the inversed thickness of the IPN ion
286 gel membrane (Fig. 3(b)). From the slope of the straight line in Fig. 3(b), the CO_2
287 permeability of the IPN ion gel membrane was determined as 747.2 barrer.
288

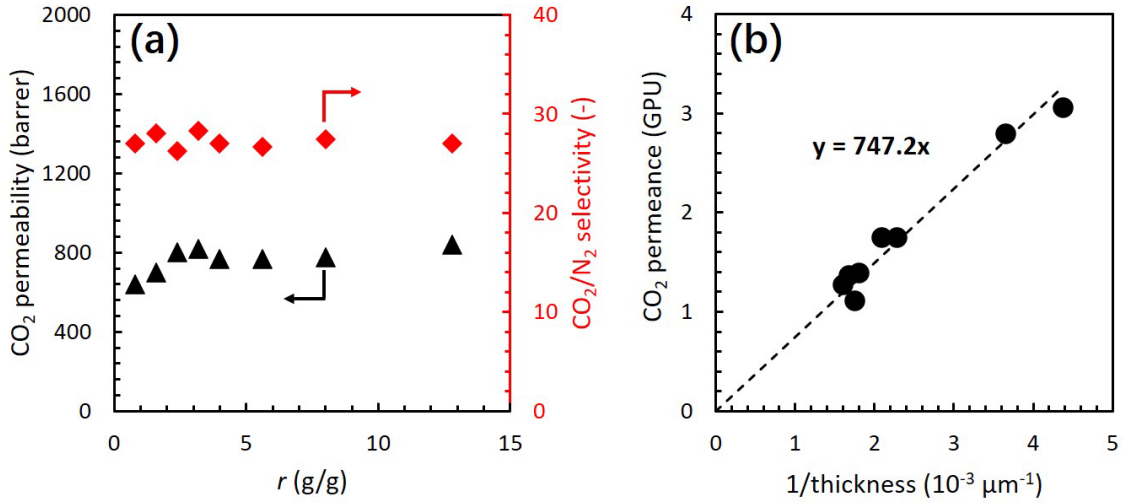

289
290 **Fig. 3.** CO_2 permeation properties of IPN ion gel membranes prepared using precursor solutions with
291 different dilution ratios. (a) Effects of dilution ratio on the CO_2 permeability and CO_2/N_2
292 permselectivity and (b) Relationship between the CO_2 permeance and inversed thickness of the IPN
293 ion gel membrane. The IL contents of the IPN ion gel membranes were 80 wt.%. The gas permeation
294 performance was evaluated at 30 °C under dry and atmospheric pressure condition.
295

296 **3.3 Optimization of the gutter layer for the preparation of the composite membrane**

297 As indicated previously, the IPN ion gel membrane provides the high mechanical

298 strength, low surface roughness, and high and selective CO_2 permeability even when a
299 highly diluted precursor solution is used. Hence, subsequently, the composite membrane
300 composed of porous support membrane, PDMS gutter layer, and the thin IPN ion gel layer
301 was prepared using the highly diluted precursor solution of the IPN ion gel. The IPN ion
302 gel precursor solutions with different *r* values were spin-coated onto the PDMS gutter
303 layers of the support membranes to prepare the composite membranes. The IL content of
304 the IPN ion gel layer was 80 wt.%.

305 First, the composite membrane was prepared by spin-coating the precursor solution
306 onto the as-prepared PDMS gutter layer without any surface treatment. The gas
307 permeation performance of the composite membranes is presented in Fig. S3(a). The CO_2
308 and N_2 permeances of the composite membrane increase with increasing *r* values, but the
309 CO_2/N_2 permselectivity dramatically decreases as a result of severe defect formation, as
310 shown in Fig. S3(b).

311 It was considered that the defect formation was attributed to the poor wettability
312 between the surface of the as-prepared PDMS gutter layer and the precursor solution of
313 the IPN ion gel. As shown in Fig. 4, at the data point corresponding to a plasma treatment
314 time of 0 seconds, the contact angle of [Emim][Tf_2N] on the as-prepared PDMS gutter
315 layer is very high (approximately 80°). Because the diluent (acetone) is highly volatile, it
316 was removed rapidly from the precursor solution after spin-coating onto the PDMS gutter
317 layer. The evaporation of the diluent caused the deterioration of the surface wettability,
318 resulting in the defect formation in the IPN ion gel layer. Therefore, to improve the

319 wettability, the PDMS gutter layer was treated by air plasma before the formation of the
320 IPN ion gel layer. As shown in Fig. 4(a), the contact angles of not only the precursor
321 solution of the IPN ion gel but also [Emim][Tf_2N] on the PDMS gutter layer effectively
322 decreased with increasing plasma treatment time. As shown in Fig. 4(b), even when the
323 plasma treatment was conducted at only 2 s, the visible defects disappeared. Therefore, it
324 is confirmed that the plasma treatment is effective in preventing the defect formation in
325 the thin IPN ion gel layer.

326 However, on the other hand, it is well known that the plasma treatment affects the gas
327 permeation performance of the PDMS gutter layer [45, 54]. Thus, to determine the
328 optimal plasma treatment time in terms of wettability and gas permeation property, the
329 effects of plasma treatment time on the CO_2 and N_2 permeation properties of the PDMS
330 gutter layer and composite membrane were evaluated. The results are presented in Figs.
331 4(c) and (d). Regarding the PDMS gutter layer, along with the increase in the plasma
332 treatment time, the CO_2 permeance decreased, but the CO_2/N_2 permselectivity slightly
333 increased. This is because of the decrease in the free volume in the gutter layer caused by
334 the conversion of the polysiloxane structure into the SiO_x structure following plasma
335 treatment [55–57].

336 It has been reported that the CO_2/N_2 permselectivity of PDMS membranes is between
337 5 and 10 [58, 59]. Thus, the CO_2/N_2 permselectivity of the PDMS gutter layers presented
338 in Fig. 4(d) indicates that no significant defects were formed in the PDMS gutter layer as
339 a result of the plasma irradiation. On the other hand, as for the composite membrane, the

340 CO_2/N_2 permselectivity significantly increases from 12 for the as-prepared membrane to
341 20 after 2 s of the plasma treatment. This improvement in the CO_2/N_2 permselectivity of
342 the composite membrane was because no defects were formed in the IPN ion gel layer
343 fabricated on the plasma-treated PDMS gutter layer. When the plasma treatment time
344 exceeds 2 s, the CO_2/N_2 permselectivity remains almost constant. Therefore, it was
345 determined that 2 s of the plasma treatment is sufficient to form the defect-free IPN ion
346 gel layer on the PDMS gutter layer. The CO_2 permeance of the composite membranes
347 monotonically decreases with increasing plasma treatment time. This is because the CO_2
348 permeance of the PDMS gutter layer decreases with increasing plasma treatment time,
349 indicating that the diffusion of the dissolved gases in the PDMS gutter layer strongly
350 affects to the overall gas permeation of the composite membrane. Therefore, from the
351 perspective of CO_2 permeability, a shorter plasma treatment duration is preferable. Based
352 on these results, the optimal plasma treatment time of the PDMS gutter layer should be 2
353 s.
354

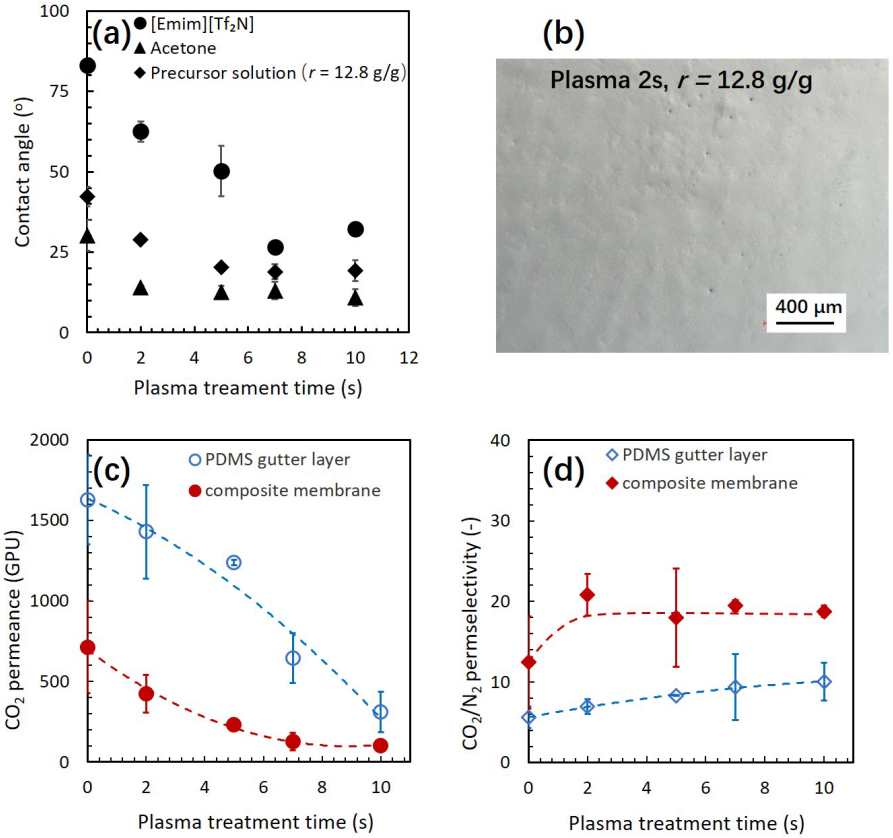

Fig. 4. Effects of the plasma treatment time on the PDMS gutter layer. (a) The contact angles of the [Emim][Tf_2N], acetone, and ion gel precursor solution on the PDMS gutter layer, (b) Surface morphology of the composite membrane prepared on the PDMS gutter layer treated by air plasma for 2s, and (c) CO_2 permeance and (d) CO_2/N_2 permselectivity of the PDMS gutter layer and the composite membrane. The precursor solution with *r* equal to 12.8 g/g was used. The weight percentage of the IL/(polymers and IL) in the precursor solution and IPN ion gel was 80 wt.%. The gas permeation performance was evaluated at 30 °C under dry and atmospheric pressure condition.

3.4 Gas permeation performance of the composite membrane with the thin IPN ion gel layer prepared using highly diluent precursor solution

A composite membrane with the thin IPN ion gel layer was fabricated using the PDMS gutter layer treated by plasma for 2 s, and the CO_2 and N_2 permeances and CO_2/N_2 permselectivities were evaluated. To prepare the composite membrane, the IPN ion gel precursor solutions with different *r* values were used to control the gel layer thickness. It

should be noted that when the *r* values were higher than 24 g/g, obvious defects were formed on the surface of the ion gel layer. Thus the highest *r* value investigated in this experiment was 24 g/g. The results of the gas permeation test are presented in Fig. 5. As shown in Fig. 5(a), the CO_2 permeance effectively increases from 45 to 613 GPU as the dilution ratio of the precursor solution increases. This monotonic increase would be due to the decrease of the ion gel layer thickness. On the other hand, the CO_2/N_2 permselectivity decreases slightly with increasing dilution ratios. Although the decrease in the CO_2/N_2 permselectivity might be caused by the defect formation in the IPN ion gel layer, the surface morphology of the IPN ion gel layer formed using the precursor solution with r = 24 g/g was very smooth and free of defects (Fig. 5(b)). Thus, it was considered that the defect formation in the IPN ion gel layer was not the reason of the decrease of the CO_2/N_2 permselectivity. The other possible reason for the decrease in the CO_2/N_2 permselectivity is the increment of the contribution of the PDMS gutter layer to total gas permeation resistance of the composite membrane along with the decrease in the IPN ion gel layer thickness. To assess the validity of this assumption, we conducted theoretical investigation of the decline of the CO_2/N_2 permselectivity.

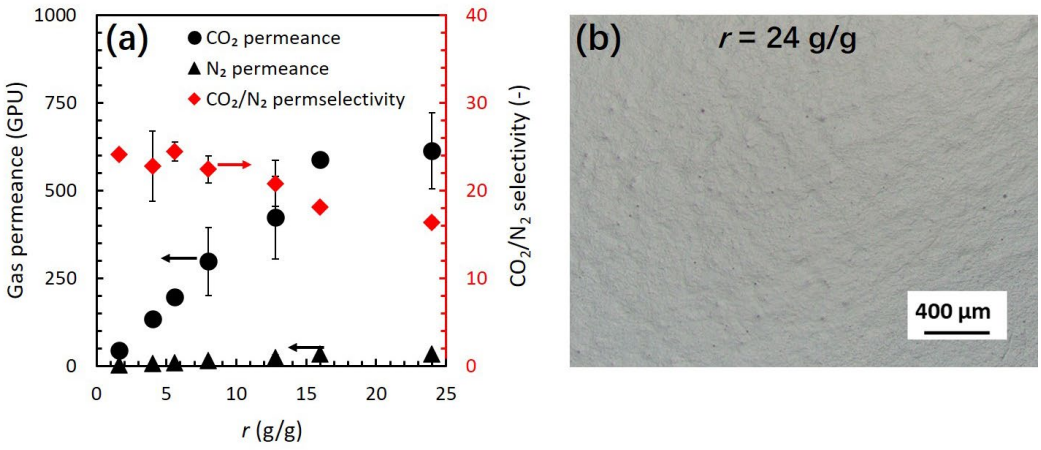

Fig. 5. CO_2 and N_2 permeation performances of the composite membrane with plasma treated PDMS gutter layer and IPN ion gel layer. (a) Effect of dilution ratio on the CO_2 and N_2 permeances and CO_2/N_2 permselectivity and (b) surface morphology of the composite membrane with the IPN ion gel layer prepared using the precursor solution with *r* equal to 24 g/g. The PDMS gutter layer treated by air plasma for 2 s was used. The IL content of the IPN ion gel layer was 80 wt.%.

The gas permeation performance of a composite membrane can be estimated using resistance model [60]. The composite membrane fabricated in this study is composed of a selective IPN ion gel layer (layer 1), a PDMS gutter layer (layer 2) and a porous PTFE support membrane (layer 3). In these diffusion resistance layers, the gas transport resistance of the porous support membrane can be ignored. Therefore, the permeance of gas species "*i*" through the composite membrane, denoted as $R_{\mathrm{i,total}}$, can be expressed by Eq. 1 [45].

$$R_{\mathrm{i,total}} = \frac{1}{\left(\frac{\delta_1}{P_{\mathrm{i},1}} + \frac{1}{R_{\mathrm{i},2}}\right)} \qquad (1)$$

Here *R* and *P* are the permeance and permeability, respectively. δ_1 is the thickness of the IPN ion gel layer. The subscript "i" represents the gas permeate (i.e., CO_2 or N_2). The subscripts "total", "1", and "2" represent the composite layer of the PDMS and IPN ion

405 gel layers, IPN ion gel layer, and PDMS layer, respectively. The permselectivity of the
406 composite membrane, denoted as S_{total}, can be expressed by Eq. 2.

407 $$S_{\text{total}} = \frac{R_{\text{CO}_2,\text{total}}}{R_{\text{N}_2,\text{total}}} = \frac{\left(\frac{\delta_1}{P_{\text{N}_2,1}} + \frac{1}{R_{\text{N}_2,2}}\right)}{\left(\frac{\delta_1}{P_{\text{CO}_2,1}} + \frac{1}{R_{\text{CO}_2,2}}\right)} \quad (2)$$

408 From Eqs. 1 and 2, Eq. 3 can be derived.

409 $$S_{\text{total}} = S_1 \cdot \left(1 - \frac{R_{\text{CO}_2,\text{total}}}{R_{\text{CO}_2,\,2}}\right) + \frac{R_{\text{CO}_2,\text{total}}}{R_{\text{N}_2,2}} \quad (3)$$

410 Here S_1 is the CO_2/N_2 permselectivity of the IPN ion gel layer ($S_1 = P_{\text{CO}_2,1}/P_{\text{N}_2,1} = 27$).
411 The CO_2 permeance $R_{\text{CO}_2,2}$ and N_2 permeance $R_{\text{N}_2,2}$ of the PDMS gutter layer treated
412 by plasma for 2 s were 1400 GPU and 238 GPU, respectively (See Figs. 4(c) and (d)).
413 Therefore, if both the ion gel layer and the gutter layer are defect-free, the relationship
414 between $R_{\text{CO}_2,\text{total}}$ and S_{total} can be estimated using Eq. 3.

415 The estimated result is presented in Fig. 6 along with the experimental data shown in
416 Fig. 5(a). As shown in this figure, the estimated curve is in good agreement with the
417 experimental results. It is worth noting that the theoretically estimated CO_2/N_2
418 permselectivity of the composite membrane decreases with the increase in the CO_2
419 permeance of the composite membrane $R_{\text{CO}_2,\text{total}}$. In other words, the theoretical
420 calculation indicates that the permselectivity decreases with the increasing $R_{\text{CO}_2,\text{total}}$,
421 even if the IPN ion gel layer has no defects. The reason for the decrease in the estimated
422 permselectivity is because the permselectivity of the PDMS gutter layer is as low as
423 approximately 6 (Fig. 4(d)) and the contribution of the PDMS gutter layer resistance to

the total resistance becomes large with the increase in the IPN ion gel layer permeance. Therefore, based on the analysis by the theoretical model (Eq. 3), it is strongly suggested that the IPN ion gel layer formed on the plasma treated PDMS gutter layer were defect-free. In other words, it is confirmed that a composite membrane with defect-free IPN ion gel layer was successfully formed using a highly diluted precursor solution.

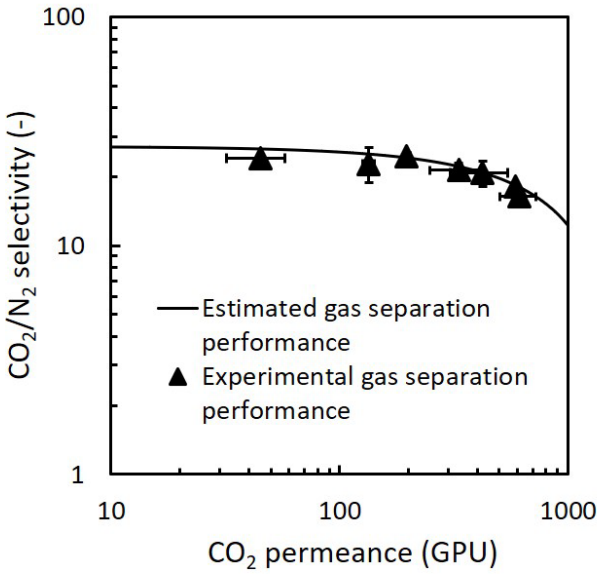

Fig. 6. Theoretically estimated relationship between the CO_2/N_2 permselectivity and the CO_2 permeance of the composite membrane. The experimental data are also plotted to compare the correlation between the estimated result with the experimental data. The composite membranes were prepared by spin-coating the precursor solutions with different dilution ratios onto the PDMS gutter layer treated by plasma for 2 s. The experimental results are the same as those shown in Fig. 5(a). The estimated curve was calculated by Eq. 3.

The ion gel layer thicknesses of the composite membranes were measured using SEM and are presented in Figs. 7(a) and 7(b). The thickness significantly decreases from 20 μm to 600 nm when the *r* value increases from 1.6 to 24 g/g. This result indicates that

increasing the dilution ratio of the precursor solution effectively reduces the thickness of the IPN ion gel layer. To confirm the reliability of the thickness of the thin ion gel layer formed using highly diluted precursor solution, we also conducted theoretical investigation. Based on Eqs. 1 and 2, we can estimate the CO_2 permeance and CO_2/N_2 permselectivity of the composite membrane with the ion gel layer with different thickness δ_1. The relationships between the CO_2 permeance and CO_2/N_2 permselectivity, and the ion gel layer thickness are presented in Figs. 7(c) and 7(d). In the calculation, it was considered that both the ion gel layer and gutter layer are defect-free. In addition, it is considered that the gas permeabilities of the IPN ion gel layer are independent on the gel layer thickness, because the IPN ion gel membrane is not a facilitated transport membrane. The CO_2 and N_2 permeabilities of the IPN ion gel layer were respectively fixed at 747.2 barrer and 27.67 barrer, which were determined for the self-standing thick ion gel membranes (see Fig. 3). The CO_2 and N_2 permeances of the PDMS gutter layer were respectively fixed at 1400 and 238 GPU (see Figs. 4(c) and 4(d)). In Figs. 7(c) and 7(d), the experimentally determined CO_2 permeances and CO_2/N_2 permselectivities of the composite membranes shown in Figs. 7(a) and 7(b) are plotted, respectively. The estimated results are in good agreement with the experimental data, indicating that the thicknesses of the IPN ion gel layers measured in Figs. 7(a) and 7(b) are reasonable. Therefore, it is confirmed that a composite membrane with an ultrathin and defect-free IPN ion gel layer can be successfully formed using a highly diluted precursor solution.

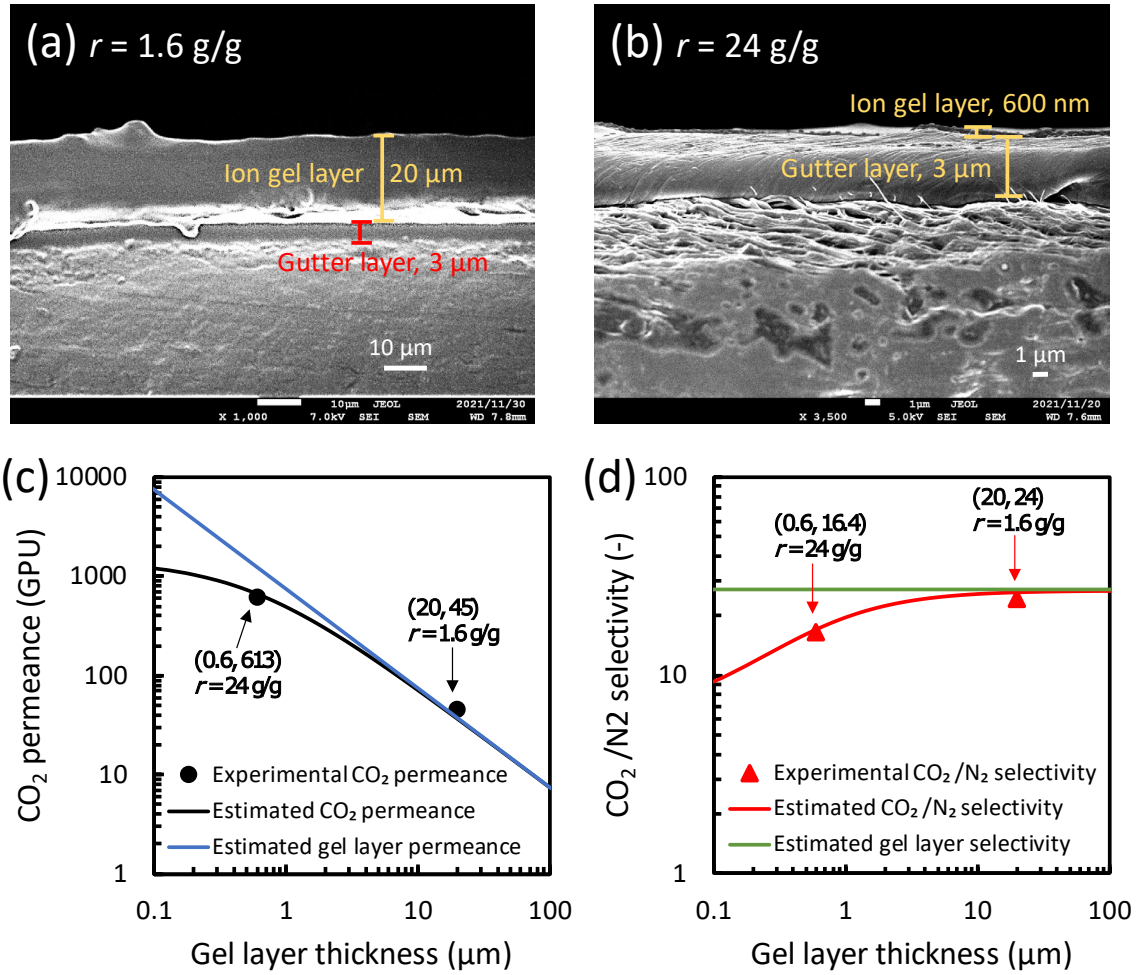

Fig. 7. The IPN ion gel layer thickness of the composite membrane. SEM images of the cross section of the composite membranes with the IPN ion gel layer prepared using the precursor solution with *r* equal to (a) 1.6 g/g and (b) 24 g/g. The composite membranes were prepared using the support membrane with the PDMS gutter layer treated by plasma for 2 s. Relationships between the (c) CO_2 permeance and (d) CO_2/N_2 permselectivity of the composite membranes, and the ion gel layer thickness. The estimated CO_2 permeance and CO_2/N_2 permselectivity of the composite membranes in parts (c) and (d) were calculated from Eqs. 1 and 2, respectively.

3.5 Gas permeation performance of the composite membrane having thin IPN ion gel layer with high IL content

Reducing the thickness of the IPN ion gel layer is an effective method for increasing

475 the CO_2 permeance of the composite membrane. On the other hand, increasing the CO_2
476 permeability of the ion gel layer is another promising method for increasing the CO_2
477 permeance of the composite membrane. The gas permeability of the IPN ion gel
478 membrane can be increased by increasing the IL content [51]. Therefore, to improve the
479 gas permeation performance of the composite membrane, the IL content of the IPN ion
480 gel layer was increased from 80 to 90 wt.%. The effect of the IL content of the IPN ion
481 gel layer on the gas permeation performance of the composite membrane is presented in
482 Figs. 8(a) and (b). As shown in Fig. 8(a), the CO_2 permeance of the composite membrane
483 effectively increases with the increasing IL content and dilution ratio. In contrast, the
484 CO_2/N_2 permselectivity decreases with the increasing IL content and the dilution ratio
485 (Fig. 8(b)). The effects of the dilution ratio on the CO_2 permeance and CO_2/N_2
486 permselectivity are the same as those for the composite membrane having the IPN ion gel
487 layer with the IL content of 80 wt.%.

488 Regarding the effect of the IL content on the CO_2 permeance, the CO_2 permeance of
489 the composite membrane increases due to the increase in the CO_2 permeability of the IPN
490 ion gel layer with the increasing IL content. The CO_2/N_2 permselectivity decreases with
491 the increasing IL content when the *r* value was over 12.8 g/g. This decrease was caused
492 by the increasing contribution of the PDMS gutter layer resistance to the total resistance
493 as a result of the increasing CO_2 permeability of the IPN ion gel layer (Eq. 3). The
494 experimental CO_2/N_2 permselectivities and the CO_2 permeances of the composite
495 membranes with different IL contents prepared using the precursor solutions with

different dilution ratios were compared with those estimated using Eq. 3 (Fig. 8(c)). The results clearly show that the experimental and theoretically estimated results are in good agreement. The good agreement indicates that the formed IPN ion gel layer with 90 wt.% of the IL content had no defect, which was also confirmed by the surface observation of the composite membrane (Fig. 8(d)). Therefore, it is demonstrated that increasing the IL content of the IPN ion gel layer is effective in increasing the CO_2 permeance of the composite membrane.

The thickness of the gel layer with 90 wt.% IL could be determined from the experimental result and Eq. 1. The CO_2 permeance of the composite membrane having the IPN ion gel layer with 90 wt.% of the IL were 778 GPU (Fig. 8(a)). In our previous work, we determined the CO_2 permeability and the CO_2/N_2 permselectivity of the self-standing IPN ion gel membrane with 90 wt.% of the IL as 1116 barrer and 27, respectively [51]. The CO_2 permeance of the plasma treated PDMS gutter layer was 1400 GPU (Fig. 4(c)). Using these values and Eq. 1, the thickness of the IPN ion gel layer of the composite membrane having the IPN ion gel layer with 90 wt.% of the IL was determined to be 600 nm. In addition, long-term stability test of the composite membrane was performed. The result is presented in Fig. 9. As shown in Fig. 9, the composite membrane with the very thin ion gel layer exhibited a good long-term stability. Thus, it was confirmed that an ultra-thin IPN ion gel layer having sufficient stability was successfully prepared even if the IL content in the gel layer was 90 wt.%.

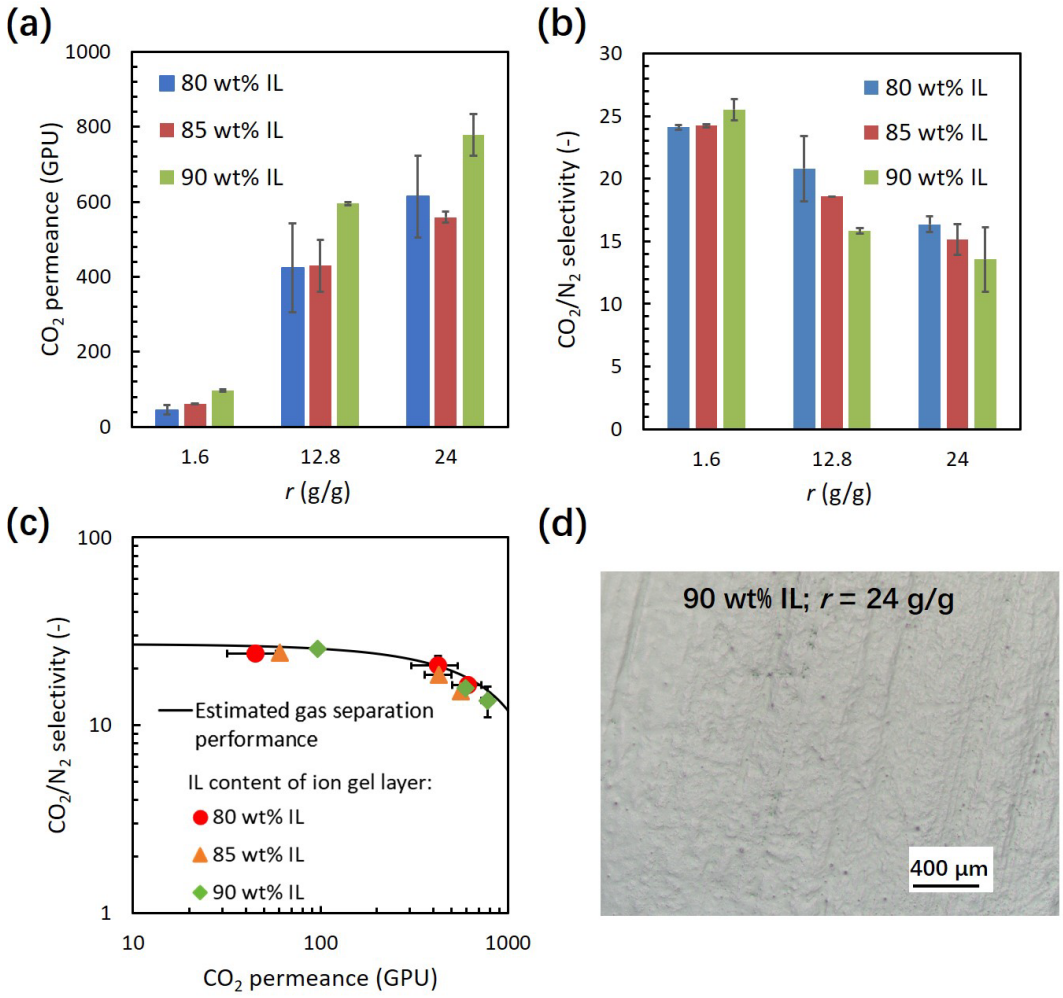

517

518 **Fig. 8.** Effect of the IL content of the IPN ion gel layer on the (a) CO_2 permeance and (b) CO_2/N_2
519 permselectivity of the composite membranes prepared using the precursor solution with different *r*
520 values. The PDMS gutter layer treated by plasma for 2 s was used to prepare the composite membranes.
521 (c) Comparison between the experimental data and the theoretically estimated relationship between
522 the CO_2/N_2 selectivity and the CO_2 permeance of the composite membranes with the IPN ion gel layer
523 having different IL contents. The estimated line was calculated by Eq. 3. (d) Surface morphology of
524 the composite membrane having the IPN ion gel layer with 90 wt.% of the IL prepared using the
525 precursor solution with *r* equal to 24 g/g.

526

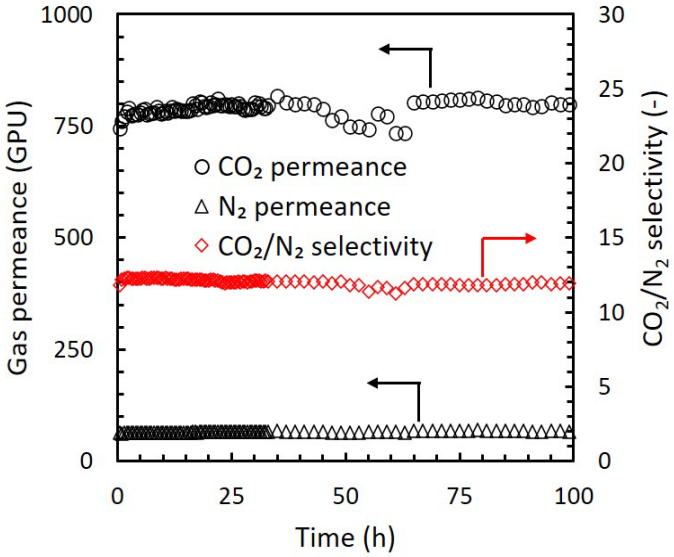

Fig. 9. Long-term stability of the IPN ion gel-based composite membrane. The IPN ion gel layer was prepared using the precursor solution with *r* equal to 24 g/g. The PDMS gutter layer treated by air plasma for 2 s was used. The IL content of the IPN ion gel layer was 90 wt.%. The gas permeation performance was evaluated at 30 °C under dry and atmospheric pressure condition.

Using the determined thickness and the CO_2 permeability of the IPN ion gel layer, the CO_2 permeance of the IPN ion gel layer was calculated to be 1860 GPU. The CO_2 permeance of 1860 GPU and the CO_2/N_2 permselectivity of 27 of the IPN ion gel layer are higher than those of the gutter layer (1400 GPU and 6, respectively). This means the insufficient CO_2 permeance of the PDMS gutter layer severely restricted the total CO_2 separation performance of the composite membrane.

3.6 Estimation of the CO_2 permeation performance of the composite membrane with a high-performance gutter layer

As mentioned above, the CO_2 permeance of the gutter layer considerably affects the overall CO_2 permeance of the composite membrane with a highly CO_2 permeable thin

IPN ion gel layer. Unfortunately, in the current stage, because it is difficult for us to prepare a highly CO_2 permeable gutter layer, the highest CO_2 permeance of our developed composite membrane was 778 GPU, which is still less than 1000 GPU. However, in recent years, the development of gutter layers has been progressing, and some state-of-the-art gutter layers have very high CO_2 permeance of even over 8000 GPU while the CO_2/N_2 permselectivity could be maintained from 7 to 11 [53, 61–69]. If a high-performance gutter layer could have been used to prepare our proposed composite membrane, there is no doubt that the CO_2 permeance of the composite membrane with the best IPN ion gel layer developed in this work should be very high. Here, we estimated the performance of the composite membrane with high performance gutter layer.

Fig. 10 presents the effects of the IPN ion gel layer thickness on the CO_2 permeance and CO_2/N_2 permselectivity of the composite membrane composed of the gutter layer with different CO_2 permeance and the IPN ion gel layer containing 90 wt.% of the IL. The CO_2 permeance and the CO_2/N_2 permselectivity of the composite membrane could be effectively improved by increasing the CO_2 permeance of the gutter layer. If the CO_2 permeance of the PDMS gutter layer is greater than 5000 GPU, then the CO_2 permeance and CO_2/N_2 permselectivity of the composite membrane with an experimentally achieved IPN ion gel layer with thickness of 600 nm could be more than 1355 GPU and over 22, respectively. These performances satisfy the requirement of the CO_2 capture for the flue gas from the coal-fired power plant (>1000 GPU CO_2 permeance and >20 CO_2/N_2 permselectivity [5]).

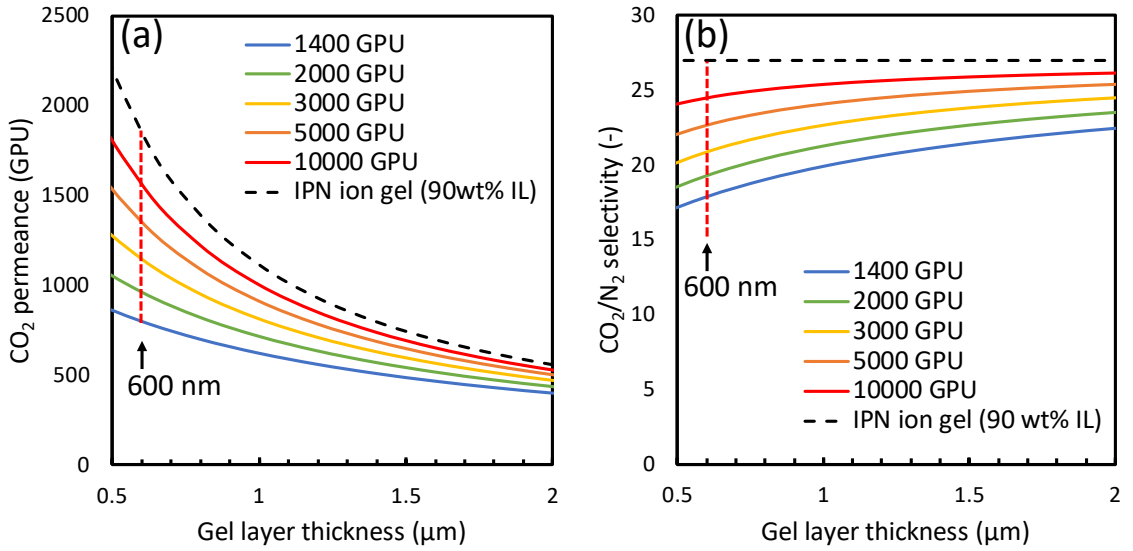

Fig. 10. Effect of gel layer thickness on the CO_2 permeance and CO_2/N_2 permselectivity of the composite membrane composed of the gutter layer with different CO_2 permeance and the IPN ion gel layer containing 90 wt.% of the IL. (a) CO_2 permeance estimated by Eq. 1 and (b) CO_2/N_2 permselectivity estimated by Eq. 2. For the calculation, the CO_2 permeability and CO_2/N_2 permselectivity of the IPN ion gel layer were fixed at 1116 barrer and 27, respectively. The CO_2/N_2 permselectivity of the PDMS gutter layer was fixed at 11.

Furthermore, using a CO_2-philic ionic liquid is another effective way to improve the performance of the composite membrane. For example, 1-ethyl-3-methylimidazolium tetracyanoborate ([Emim][$B(CN)_4$]) is a promising ionic liquid. It was reported that the supported ionic liquid membrane (SILM) with [Emim][$B(CN)_4$] had the high CO_2 permeability of 2040 barrer and CO_2/N_2 selectivity of 53 [70]. If a [Emim][$B(CN)_4$]-based thin IPN ion gel layer (600 nm) with the similar CO_2 separation performance to the SILM can be formed on the PDMS gutter layer with 5000 GPU of the CO_2 permeance and 11 of the CO_2/N_2 selectivity, it can be estimated that the composite membrane could have 2000 GPU of the CO_2 permeance and 36 of the CO_2/N_2 selectivity. In accordance with the simulated result by Merkel *et al.* [5], the performance of this hypothetical

583 membrane is sufficient for the feasible process design of a CO_2 capture from a coal-fired
584 power plant exhaust gas. Thus, it can be considered that the ion gel-based composite
585 membrane has the potential to be used for the CO_2 capture application. However, it is true
586 the CO_2/N_2 permselectivity of the composite membrane (36) is still insufficient to recover
587 the permeate with high CO_2 purity (e.g. more than 90%) at more than 90% of CO_2
588 recovery. In other words, to establish an efficient carbon capture and storage (CCS)
589 system, a single-stage process using the hypothetical ion gel-based composite membrane
590 would be still insufficient; *i.e.* a multi-stage membrane process or a hybrid process
591 combining the membrane unit with another separation unit such as a cryogenic distillation,
592 absorption, or adsorption unit should be considered. Considering CCS, single-stage
593 membrane process would be insufficient, but still using high performance CO_2 separation
594 membrane is meaningful. Using a high performance CO_2 separation membrane enables
595 to reduce the total cost of the CO_2 capture process.

596 As mentioned above, many opportunities to improve the CO_2 separation performance
597 of the IPN ion gel-based composite membrane still remain. It is expected that the
598 optimization of the gutter layer and ion gel layer would provide feasible and desirable
599 CO_2 separation membranes for the practical CO_2 separation process.

600

601 **4. Conclusion**

602 A composite membrane with an ultra-thin (thickness of 600nm) and defect-free IPN
603 ion gel layer was prepared on a PDMS gutter layer via spin-coating. The thickness of the

IPN ion gel layer was significantly reduced from 20 μm to 600 nm by increasing the dilution ratio of the IPN ion gel precursor solution. Based on the high mechanical strength and good IL holding property of the IPN ion gel, the ultra-thin and defect-free IPN ion gel layer with up to 90 wt.% of the IL was successfully prepared. The CO_2 permeance of the composite membrane was effectively improved from 45 to 778 GPU by decreasing the thickness and increasing the IL content of the IPN ion gel layer. Through theoretical analysis, it was confirmed that the CO_2 permeance and the CO_2/N_2 selectivity of the IPN ion gel layer with the thickness of 600 nm and the IL content of 90 wt.% were determined as 1860 GPU and 27, respectively. The estimation of the CO_2 separation performance of the composite membrane with a high-performance gutter layer and the IPN ion gel layer indicated that the IPN gel is a good optional material as a selective layer of a composite membranes for efficient CO_2 separation.

Acknowledgment

This work was partly supported by KAKENHI (21H01691) of the Japan Society for the Promotion of Science (JSPS) and by the China Scholarship Council (CSC) (Jinhui Zhang).

References

[1] B. Ekwurzel, J. Boneham, M. Dalton, R. Heede, R.J. Mera, M.R. Allen, P.C. Frumhoff, The rise in global atmospheric CO_2, surface temperature, and sea level from emissions

625 traced to major carbon producers, Clim. Change 144(4) (2017) 579-590.
626 https://doi.org/10.1007/s10584-017-1978-0.
627 [2] M.Z. Jacobson, Review of solutions to global warming, air pollution, and energy
628 security, Energy Environ. Sci. 2(2) (2009) 148-173. https://doi.org/10.1039/B809990C.
629 [3] H.A. Patel, J. Byun, C.T. Yavuz, Carbon Dioxide Capture Adsorbents: Chemistry and
630 Methods, ChemSusChem 10(7) (2017) 1303-1317.
631 https://doi.org/10.1002/cssc.201601545.
632 [4] R. Khalilpour, K. Mumford, H. Zhai, A. Abbas, G. Stevens, E.S. Rubin, Membrane-
633 based carbon capture from flue gas: a review, J. Clean. Prod. 103 (2015) 286-300.
634 https://doi.org/10.1016/j.jclepro.2014.10.050.
635 [5] T.C. Merkel, H. Lin, X. Wei, R. Baker, Power plant post-combustion carbon dioxide
636 capture: An opportunity for membranes, J. Membr. Sci. 359(1-2) (2010) 126-139.
637 https://doi.org/10.1016/j.memsci.2009.10.041.
638 [6] Y. Ding, Perspective on gas separation membrane materials from process economics
639 point of view, Ind. Eng. Chem. Res. 59(2) (2019) 556-568.
640 https://doi.org/10.1021/acs.iecr.9b05975.
641 [7] S. Wang, X. Li, H. Wu, Z. Tian, Q. Xin, G. He, D. Peng, S. Chen, Y. Yin, Z. Jiang,
642 Advances in high permeability polymer-based membrane materials for CO_2 separations,
643 Energy Environ. Sci. 9(6) (2016) 1863-1890. https://doi.org/10.1039/C6EE00811A.
644 [8] R.W. Baker, B.T. Low, Gas Separation Membrane Materials: A Perspective,
645 Macromolecules 47(20) (2014) 6999-7013. https://doi.org/10.1021/ma501488s.

[9] T.K. Carlisle, G.D. Nicodemus, D.L. Gin, R.D. Noble, CO_2/light gas separation performance of cross-linked poly (vinylimidazolium) gel membranes as a function of ionic liquid loading and cross-linker content, J. Membr. Sci. 397 (2012) 24-37. https://doi.org/10.1016/j.memsci.2012.01.006.

[10] F. Moghadam, E. Kamio, H. Matsuyama, High CO_2 separation performance of amino acid ionic liquid-based double network ion gel membranes in low CO_2 concentration gas mixtures under humid conditions, J. Membr. Sci. 525 (2017) 290-297. https://doi.org/10.1016/j.memsci.2016.12.002.

[11] F. Moghadam, E. Kamio, T. Yoshioka, H. Matsuyama, New approach for the fabrication of double-network ion-gel membranes with high CO_2/N_2 separation performance based on facilitated transport, J. Membr. Sci. 530 (2017) 166-175. https://doi.org/10.1016/j.memsci.2017.02.032.

[12] F. Moghadam, E. Kamio, A. Yoshizumi, H. Matsuyama, An amino acid ionic liquid-based tough ion gel membrane for CO_2 capture, Chem Commun (Camb) 51(71) (2015) 13658-61. https://doi.org/10.1039/c5cc04841a.

[13] B. Sasikumar, G. Arthanareeswaran, A. Ismail, Recent progress in ionic liquid membranes for gas separation, J. Mol. Liq. 266 (2018) 330-341. https://doi.org/10.1016/j.molliq.2018.06.081.

[14] K. Xie, Q. Fu, G.G. Qiao, P.A. Webley, Recent progress on fabrication methods of polymeric thin film gas separation membranes for CO_2 capture, J. Membr. Sci. 572 (2019) 38-60. https://doi.org/10.1016/j.memsci.2018.10.049.

667 [15] H. Matsuyama, M. Teramoto, H. Sakakura, K. Iwai, Facilitated transport of CO_2
668 through various ion exchange membranes prepared by plasma graft polymerization, J.
669 Membr. Sci. 117(1-2) (1996) 251-260. https://doi.org/10.1016/0376-7388(96)00072-5.
670 [16] H. Matsuyama, K. Matsui, Y. Kitamura, T. Maki, M. Teramoto, Effects of membrane
671 thickness and membrane preparation condition on facilitated transport of CO_2 through
672 ionomer membrane, Sep. Purif. Technol. 17(3) (1999) 235-241.
673 https://doi.org/10.1016/S1383-5866(99)00047-7.
674 [17] M. Zia ul Mustafa, H. bin Mukhtar, N.A.H. Md Nordin, H.A. Mannan, R. Nasir, N.
675 Fazil, Recent Developments and Applications of Ionic Liquids in Gas Separation
676 Membranes, Chem. Eng. Technol. 42(12) (2019) 2580-2593.
677 https://doi.org/10.1002/ceat.201800519.
678 [18] L.C. Tome, I.M. Marrucho, Ionic liquid-based materials: A platform to design
679 engineered CO_2 separation membranes, Chem. Soc. Rev. 45(10) (2016) 2785-2824.
680 https://doi.org/10.1039/c5cs00510h.
681 [19] Z. Dai, R.D. Noble, D.L. Gin, X. Zhang, L. Deng, Combination of ionic liquids with
682 membrane technology: A new approach for CO_2 separation, J. Membr. Sci. 497 (2016) 1-
683 20. https://doi.org/10.1016/j.memsci.2015.08.060.
684 [20] M. Hasib-ur-Rahman, M. Siaj, F. Larachi, Ionic liquids for CO_2 capture—
685 development and progress, Chem. Eng. Process.: Process Intensif. 49(4) (2010) 313-322.
686 https://doi.org/10.1016/j.cep.2010.03.008.
687 [21] Z. Lei, C. Dai, B. Chen, Gas solubility in ionic liquids, Chem. Rev. 114(2) (2014)

688 1289-1326. https://doi.org/10.1021/cr300497a.
689 [22] M.J. Muldoon, S.N. Aki, J.L. Anderson, J.K. Dixon, J.F. Brennecke, Improving
690 carbon dioxide solubility in ionic liquids, J. Phys. Chem. B 111(30) (2007) 9001-9009.
691 https://doi.org/10.1021/jp071897q.
692 [23] J. Huang, T. Rüther, Why are ionic liquids attractive for CO_2 absorption? An
693 overview, Aust. J. Chem. 62(4) (2009) 298-308. https://doi.org/10.1071/CH08559.
694 [24] C. Cadena, J.L. Anthony, J.K. Shah, T.I. Morrow, J.F. Brennecke, E.J. Maginn, Why
695 is CO_2 so soluble in imidazolium-based ionic liquids?, J. Am. Chem. Soc. 126(16) (2004)
696 5300-5308. https://doi.org/10.1021/ja039615x.
697 [25] A. Finotello, J.E. Bara, D. Camper, R.D. Noble, Room-temperature ionic liquids:
698 temperature dependence of gas solubility selectivity, Ind. Eng. Chem. Res. 47(10) (2008)
699 3453-3459. https://doi.org/10.1021/ie0704142.
700 [26] S.M. Mahurin, P.C. Hillesheim, J.S. Yeary, D.-e. Jiang, S. Dai, High CO_2 solubility,
701 permeability and selectivity in ionic liquids with the tetracyanoborate anion, RSC Adv.
702 2(31) (2012) 11813-11819. https://doi.org/10.1039/C2RA22342B.
703 [27] A. Thran, G. Kroll, F. Faupel, Correlation between fractional free volume and
704 diffusivity of gas molecules in glassy polymers, J. Polym. Sci., Part B: Polym. Phys.
705 37(23) (1999) 3344-3358. https://doi.org/10.1002/(SICI)1099-
706 0488(19991201)37:23<3344::AID-POLB10>3.0.CO;2-A.
707 [28] Y. Hirayama, Y. Kase, N. Tanihara, Y. Sumiyama, Y. Kusuki, K. Haraya, Permeation
708 properties to CO_2 and N_2 of poly (ethylene oxide)-containing and crosslinked polymer

709 films, J. Membr. Sci. 160(1) (1999) 87-99. https://doi.org/10.1016/S0376-
710 7388(99)00080-0.
711 [29] D. Morgan, L. Ferguson, P. Scovazzo, Diffusivities of gases in room-temperature
712 ionic liquids: data and correlations obtained using a lag-time technique, Ind. Eng. Chem.
713 Res. 44(13) (2005) 4815-4823.
714 [30] S.S. Moganty, R.E. Baltus, Diffusivity of carbon dioxide in room-temperature ionic
715 liquids, Ind. Eng. Chem. Res. 49(19) (2010) 9370-9376.
716 https://doi.org/10.1021/ie101260j.
717 [31] C. Moya, J. Palomar, M. Gonzalez-Miquel, J. Bedia, F. Rodriguez, Diffusion
718 coefficients of CO_2 in ionic liquids estimated by gravimetry, Ind. Eng. Chem. Res. 53(35)
719 (2014) 13782-13789. https://doi.org/10.1021/ie501925d.
720 [32] X. Yan, S. Anguille, M. Bendahan, P. Moulin, Ionic liquids combined with membrane
721 separation processes: a review, Sep. Purif. Technol. 222 (2019) 230-253.
722 https://doi.org/10.1016/j.seppur.2019.03.103.
723 [33] R.D. Noble, D.L. Gin, Perspective on ionic liquids and ionic liquid membranes, J.
724 Membr. Sci. 369(1-2) (2011) 1-4. https://doi.org/10.1016/j.memsci.2010.11.075.
725 [34] K. Fujii, T. Makino, K. Hashimoto, T. Sakai, M. Kanakubo, M. Shibayama, Carbon
726 dioxide separation using a high-toughness ion gel with a tetra-armed polymer network,
727 Chem. Lett. 44(1) (2015) 17-19. https://doi.org/doi.org/10.1246/cl.140795.
728 [35] E. Kamio, M. Minakata, Y. Iida, T. Yasui, A. Matsuoka, H. Matsuyama,
729 Inorganic/organic double-network ion gel membrane with a high ionic liquid content for

730 CO_2 separation, Polym. J. 53(1) (2020) 137-147. https://doi.org/10.1038/s41428-020-
731 0393-y.
732 [36] Y. Gu, E.L. Cussler, T.P. Lodge, ABA-triblock copolymer ion gels for CO_2 separation
733 applications, J. Membr. Sci. 423 (2012) 20-26.
734 https://doi.org/10.1016/j.memsci.2012.07.011.
735 [37] Y. Gu, T.P. Lodge, Synthesis and Gas Separation Performance of Triblock Copolymer
736 Ion Gels with a Polymerized Ionic Liquid Mid-Block, Macromolecules 44(7) (2011)
737 1732-1736. https://doi.org/10.1021/ma2001838.
738 [38] L.C. Tome, I.M. Marrucho, Ionic liquid-based materials: a platform to design
739 engineered CO_2 separation membranes, Chem. Soc. Rev. 45(10) (2016) 2785-824.
740 https://doi.org/10.1039/c5cs00510h.
741 [39] J. Zhou, M.M. Mok, M.G. Cowan, W.M. McDanel, T.K. Carlisle, D.L. Gin, R.D.
742 Noble, High-permeance room-temperature ionic-liquid-based membranes for CO_2/N_2
743 separation, Ind. Eng. Chem. Res. 53(51) (2014) 20064-20067.
744 https://doi.org/10.1021/ie5040682.
745 [40] C. Ma, M. Wang, Z. Wang, M. Gao, J. Wang, Recent progress on thin film composite
746 membranes for CO_2 separation, J. CO_2 Util. 42 (2020) 101296.
747 https://doi.org/10.1016/j.jcou.2020.101296.
748 [41] E. Kamio, T. Yasui, Y. Iida, J.P. Gong, H. Matsuyama, Inorganic/Organic Double-
749 Network Gels Containing Ionic Liquids, Adv. Mater. 29(47) (2017) 1704118.
750 https://doi.org/10.1002/adma.201704118.

751 [42] E. Kamio, M. Kinoshita, T. Yasui, T.P. Lodge, H. Matsuyama, Preparation of
752 Inorganic/Organic Double-Network Ion Gels Using a Cross-Linkable Polymer in an Open
753 System, Macromolecules 53(19) (2020) 8529-8538.
754 https://doi.org/10.1021/acs.macromol.0c01488.
755 [43] T. Yasui, S. Fujinami, T. Hoshino, E. Kamio, H. Matsuyama, Energy dissipation via
756 the internal fracture of the silica particle network in inorganic/organic double network ion
757 gels, Soft matter 16(9) (2020) 2363-2370. https://doi.org/10.1039/C9SM02174D.
758 [44] T. Yasui, E. Kamio, H. Matsuyama, Inorganic/Organic Double-Network Ion Gels
759 with Partially Developed Silica-Particle Network, Langmuir 34(36) (2018) 10622-10633.
760 https://doi.org/10.1021/acs.langmuir.8b01930.
761 [45] J. Zhang, E. Kamio, M. Kinoshita, A. Matsuoka, K. Nakagawa, T. Yoshioka, H.
762 Matsuyama, Inorganic/Organic Micro-Double-Network Ion Gel-Based Composite
763 Membrane with Enhanced Mechanical Strength and CO_2 Permeance, Ind. Eng. Chem.
764 Res. 60(34) (2021) 12698-12708. https://doi.org/10.1021/acs.iecr.1c02228.
765 [46] J. Zhang, E. Kamio, A. Matsuoka, K. Nakagawa, T. Yoshioka, H. Matsuyama,
766 Development of a Micro-Double-Network Ion Gel-Based CO_2 Separation Membrane
767 from Nonvolatile Network Precursors, Ind. Eng. Chem. Res. 60(34) (2021) 12640-12649.
768 https://doi.org/10.1021/acs.iecr.1c01529.
769 [47] K. Fujii, H. Asai, T. Ueki, T. Sakai, S. Imaizumi, U.-i. Chung, M. Watanabe, M.
770 Shibayama, High-performance ion gel with tetra-PEG network, Soft Matter 8(6) (2012)
771 1756-1759. https://doi.org/10.1039/C2SM07119C.

772 [48] Y. Gu, S. Zhang, L. Martinetti, K.H. Lee, L.D. McIntosh, C.D. Frisbie, T.P. Lodge,
773 High toughness, high conductivity ion gels by sequential triblock copolymer self-
774 assembly and chemical cross-linking, J. Am. Chem. Soc. 135(26) (2013) 9652-9655.
775 https://doi.org/10.1021/ja4051394.
776 [49] D. Weng, F. Xu, X. Li, S. Li, Y. Li, J. Sun, Polymeric Complex-Based Transparent
777 and Healable Ionogels with High Mechanical Strength and Ionic Conductivity as Reliable
778 Strain Sensors, ACS appl. mater. interfaces 12(51) (2020) 57477-57485.
779 https://doi.org/10.1021/acsami.0c18832.
780 [50] Z. Tang, X. Lyu, A. Xiao, Z. Shen, X. Fan, High-Performance Double-Network Ion
781 Gels with Fast Thermal Healing Capability via Dynamic Covalent Bonds, Chem. Mater.
782 30(21) (2018) 7752-7759. https://doi.org/10.1021/acs.chemmater.8b03104.
783 [51] J. Zhang, E. Kamio, A. Matsuoka, K. Nakagawa, T. Yoshioka, H. Matsuyama, Novel
784 Tough Ion-Gel-Based CO_2 Separation Membrane with Interpenetrating Polymer Network
785 Composed of Semicrystalline and Cross-Linkable Polymers, Ind. Eng. Chem. Res. 61(13)
786 (2022) 4648-4658. https://doi.org/10.1021/acs.iecr.1c04800.
787 [52] O. Selyanchyn, R. Selyanchyn, S. Fujikawa, Critical role of the molecular interface
788 in double-layered Pebax-1657/PDMS nanomembranes for highly efficient CO_2/N_2 gas
789 separation, ACS appl. mater. interfaces 12(29) (2020) 33196-33209.
790 https://doi.org/10.1021/acsami.0c07344.
791 [53] S. Fujikawa, M. Ariyoshi, R. Selyanchyn, T. Kunitake, Ultra-fast, selective CO_2
792 permeation by free-standing siloxane nanomembranes, Chem. Lett. 48(11) (2019) 1351-

1354. https://doi.org/10.1246/cl.190558.

[54] H. Matsuyama, M. Teramoto, K. Hirai, Effect of plasma treatment on CO_2 permeability and selectivity of poly (dimethylsiloxane) membrane, J. Membr. Sci. 99(2) (1995) 139-147. https://doi.org/10.1016/0376-7388(94)00217-M.

[55] H. Hillborg, J. Ankner, U.W. Gedde, G. Smith, H. Yasuda, K. Wikström, Crosslinked polydimethylsiloxane exposed to oxygen plasma studied by neutron reflectometry and other surface specific techniques, Polymer 41(18) (2000) 6851-6863. https://doi.org/10.1016/S0032-3861(00)00039-2.

[56] J.-T. Chen, Y.-J. Fu, K.-L. Tung, S.-H. Huang, W.-S. Hung, S.J. Lue, C.-C. Hu, K.-R. Lee, J.-Y. Lai, Surface modification of poly (dimethylsiloxane) by atmospheric pressure high temperature plasma torch to prepare high-performance gas separation membranes, J. Membr. Sci. 440 (2013) 1-8. https://doi.org/10.1016/j.memsci.2013.03.058.

[57] K. Tsuji, M. Nakaya, A. Uedono, A. Hotta, Enhancement of the gas barrier property of polypropylene by introducing plasma-treated silane coating with SiO_x-modified top-surface, Surf. Coat. Technol. 284 (2015) 377-383. https://doi.org/10.1016/j.surfcoat.2015.10.027.

[58] G.-L. Zhuang, C.-F. Wu, M.-Y. Wey, H.-H. Tseng, Impacts of Green Synthesis Process on Asymmetric Hybrid PDMS Membrane for Efficient CO_2/N_2 Separation, Membranes 11(1) (2021) 59. https://doi.org/10.3390/membranes11010059.

[59] G. Li, K. Knozowska, J. Kujawa, A. Tonkonogovas, A. Stankevičius, W. Kujawski,

814 Fabrication of Polydimethysiloxane (PDMS) Dense Layer on Polyetherimide (PEI)
815 Hollow Fiber Support for the Efficient CO_2/N_2 Separation Membranes, Polymers 13(5)
816 (2021) 756. https://doi.org/10.3390/polym13050756.
817 [60] J.M. Henis, M.K. Tripodi, Composite hollow fiber membranes for gas separation:
818 the resistance model approach, J. Membr. Sci. 8(3) (1981) 233-246.
819 https://doi.org/10.1016/S0376-7388(00)82312-1.
820 [61] R. Selyanchyn, M. Ariyoshi, S. Fujikawa, Thickness effect on CO_2/N_2 separation in
821 double layer Pebax-1657®/PDMS membranes, Membranes 8(4) (2018) 121.
822 https://doi.org/10.3390/membranes8040121.
823 [62] M. Ariyoshi, S. Fujikawa, T. Kunitake, Robust, Hyper-Permeable Nanomembrane
824 Composites of Poly (dimethylsiloxane) and Cellulose Nanofibers, ACS appl. mater.
825 interfaces 13(51) (2021) 61189-61195. https://doi.org/10.1021/acsami.1c19220.
826 [63] Q. Fu, A. Halim, J. Kim, J.M. Scofield, P.A. Gurr, S.E. Kentish, G.G. Qiao, Highly
827 permeable membrane materials for CO_2 capture, J. Mater. Chem. A 1(44) (2013) 13769-
828 13778. https://doi.org/10.1039/C3TA13066E.
829 [64] A. Halim, Q. Fu, Q. Yong, P.A. Gurr, S.E. Kentish, G.G. Qiao, Soft polymeric
830 nanoparticle additives for next generation gas separation membranes, J. Mater. Chem. A
831 2(14) (2014) 4999-5009. https://doi.org/10.1039/C3TA14170E.
832 [65] Q. Fu, E.H. Wong, J. Kim, J.M. Scofield, P.A. Gurr, S.E. Kentish, G.G. Qiao, The
833 effect of soft nanoparticles morphologies on thin film composite membrane performance,
834 J. Mater. Chem. A 2(42) (2014) 17751-17756. https://doi.org/10.1039/C4TA02859G.

[66] P. Li, Z. Wang, W. Li, Y. Liu, J. Wang, S. Wang, High-performance multilayer composite membranes with mussel-inspired polydopamine as a versatile molecular bridge for CO_2 separation, ACS appl. mater. interfaces 7(28) (2015) 15481-15493. https://doi.org/10.1021/acsami.5b03786.

[67] C.Z. Liang, T.S. Chung, Ultrahigh flux composite hollow fiber membrane via highly crosslinked PDMS for recovery of hydrocarbons: propane and propene, Macromol. Rapid Commun. 39(5) (2018) 1700535. https://doi.org/10.1002/marc.201700535.

[68] P. Li, H.Z. Chen, T.-S. Chung, The effects of substrate characteristics and pre-wetting agents on PAN–PDMS composite hollow fiber membranes for CO_2/N_2 and O_2/N_2 separation, J. Membr. Sci. 434 (2013) 18-25. https://doi.org/10.1016/j.memsci.2013.01.042.

[69] M.J. Yoo, K.H. Kim, J.H. Lee, T.W. Kim, C.W. Chung, Y.H. Cho, H.B. Park, Ultrathin gutter layer for high-performance thin-film composite membranes for CO_2 separation, J. Membr. Sci. 566 (2018) 336-345. https://doi.org/10.1016/j.memsci.2018.09.017.

[70] S.M. Mahurin, P.C. Hillesheim, J.S. Yeary, D.-e. Jiang, S. Dai, High CO_2 solubility, permeability and selectivity in ionic liquids with the tetracyanoborate anion, RSC Adv. 2(31) (2012) 11813-11819. https://doi.org/10.1039/c2ra22342b.